

Rashba control for the spin excitation of a fully spin-polarized vertical quantum dot

P. Lucignano,^{1,2} B. Jouault,³ A. Tagliacozzo,^{1,2} and B. L. Altshuler⁴

¹*Coherentia-INFM, Napoli, Italy*

²*Dipartimento di Scienza Fisiche, Università di Napoli "Federico II," Monte S. Angelo, via Cintia, I-80126 Napoli, Italy*

³*GES, UMR 5650, Université Montpellier II, 34095 Montpellier Cedex 5, France*

⁴*Physics Department, Princeton University, Princeton, New Jersey 08540, USA*

and NEC Research Institute, Princeton, New Jersey 08540, USA

(Received 3 January 2005; published 22 March 2005)

Far-infrared radiation absorption of a quantum dot with few electrons in an orthogonal magnetic field could monitor the crossover to the fully spin-polarized state. A Rashba spin-orbit coupling can tune the energy and the spin density of the first excited state that has a spin texture carrying one extra unit of angular momentum. The spin-orbit coupling can squeeze a flipped spin density at the center of the dot and can increase the gap in the spectrum.

DOI: 10.1103/PhysRevB.71.121310

PACS number(s): 73.21.La, 73.23.-b, 78.67.Hc

Introduction. Quantum dots (QD's), confining one or few active electrons,¹ have been proposed as devices for the future quantum electronics. One of the possibilities is to operate on the spin of the trapped electrons as a qubit.² In a different proposal the QD controls the nuclear spins embedded in the crystal matrix via hyperfine coupling.³ In both cases, the polarization of the spins is expected to last long enough at low temperatures, so that the quantum computation can be carried out. Controlled spin transfer between electrons and nuclei has been demonstrated to be possible in a spin-polarized two-dimensional electron gas (2DEG).⁴ In a 2DEG, fully spin-polarized quantum Hall states are used to manipulate the orientation of nuclear spins. Low-lying Skyrmin states at filling close to one are used to reset the nuclear spin system by inducing fast-spin relaxation. In the presence of a magnetic field B orthogonal to the dot, the relaxation mechanism seems to be dominated by hyperfine interaction for $B < 0.5T$ and by spin-orbit (SO) coupling assisted by phonons for higher fields.⁵

The Rashba SO interaction,⁶ which arises in QD structures from the lack of inversion symmetry caused by the two-dimensional (2D) confinement, can be controlled by gate voltages parallel to the x - y structure.⁷ This possibility has been beautifully shown in InGaAs-based 2DEG (Ref. 8)

and in a recent experiment on large lateral QD, where the conductance has been tuned from the weak localization limit, without SO coupling, to the antilocalization limit, with SO.⁹ The inverse relaxation time $1/T_1$ has also been probed recently by transport across a single QD.¹⁰

Thanks to the combined effect of e - e interactions and of an appropriate $B > B^*$ orthogonal to the dot ($\parallel \hat{z}$), the QD becomes a "maximum density droplet" (MDD) with a fully spin-polarized (FSP) ground state (GS).¹¹ In this paper we show that controlled SO interaction of a FSP QD, made out of III-V semiconductors, can be used to adiabatically modify the low-lying energy states of few ($N=2, 3, 4$) trapped electrons and their spin density (represented respectively in Figs. 1–3). The Rashba-SO coupling contributes to a well-defined collective spin excitation [first excited state (FES)], with a change of the spin density, with respect to the GS, localized at the origin of the QD. This excitation can be pumped with far-infrared radiation (FIR). Using numerical diagonalization for few electrons in the dot, we find that the absorption intensity for circularly polarized FIR is strongly enhanced when the crossover to the FSP state is completed (see Fig. 5). The spin density can be squeezed at the center of the dot by increasing the SO coupling α (see Fig. 4). Mean-

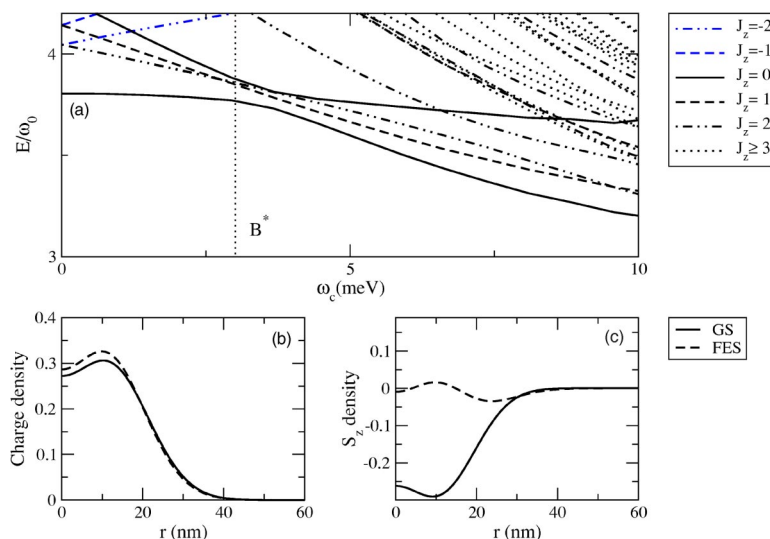


FIG. 1. (Color online) $N=2$ particles dot: (a) Energy spectrum vs magnetic field ω_c in the presence of the SO. Values of the parameters are in the text. The GS is $J_z=0$, the FES is $J_z=1$. (b) The charge densities of the GS (black line) and of the FES (dashed line) of the FSP dot. (c) Corresponding spin densities of the GS (black line) and of the FES (dashed line) of the FSP dot.

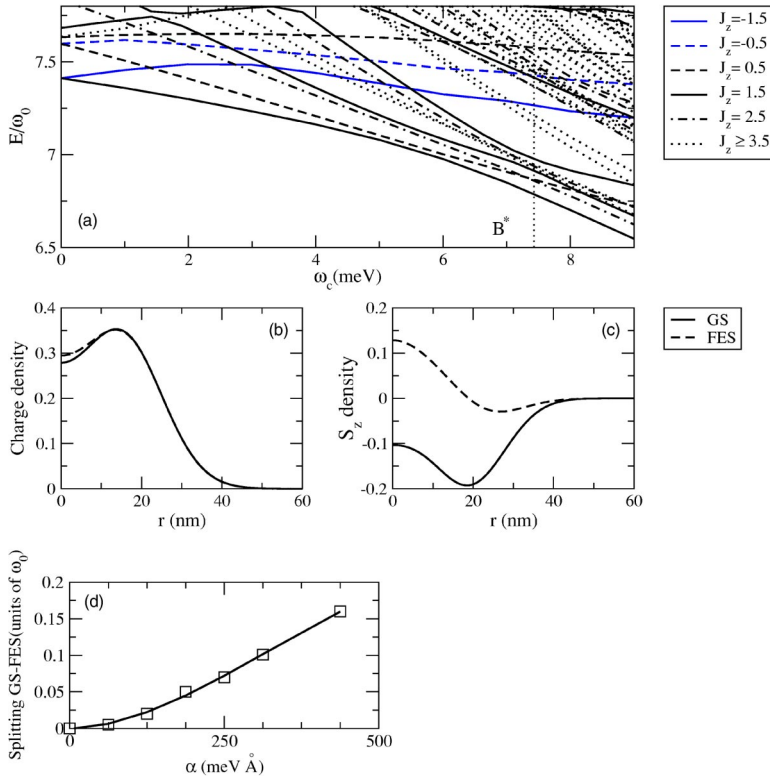


FIG. 2. (Color online) $N=3$ particles dot: (a) Energy spectrum vs magnetic field ω_c in the presence of the SO . $\omega_d=7$ meV, $U=13$ meV, $\alpha=250$ meV \AA . The GS is $J_z=3/2$, the FES is $J_z=5/2$. (b) The charge densities of the GS (black line) and of the FES (dashed line) of the FSP dot. (c) The corresponding spin densities of the GS (black line) and of the FES (dashed line) of the FSP dot. (d) The GS-FES spin gap vs α at $\omega_c=8$ meV.

while the gap between the GS and FES increases with α [as shown in Fig. 2(d)] for $N=3$.

QD spin properties tuned by SO for $B > B^*$. The electrons are confined in two dimensions (x, y) by a parabolic potential of characteristic frequency ω_d , in the presence of $\vec{B} = -B\hat{z}$. The single-particle Hamiltonian for the i th electron, in the effective mass approximation (m_e^*), is

$$H_{(i)} = \frac{1}{2m_e^*} \left(\vec{p}_i + \frac{e}{c} \vec{A}_i \right)^2 + \frac{1}{2} m_e^* \omega_d^2 r_i^2, \quad (1)$$

with $\vec{A}_i = B/2(y_i, -x_i, 0)$, and $-e$ is the electron charge.

The Zeeman spin splitting would only mask our results with additional inessential complications and we neglect it.¹²

The single-particle Darwin-Fock states ϕ_{nm} are the eigenfunctions of the 2D harmonic oscillator with frequency $\omega_o = \sqrt{\omega_d^2 + \omega_c^2}/4$, where $\omega_c = eB/m_e^*c$, the cyclotron frequency. m is the angular momentum in the z direction [$m \in (-n, -n+2, \dots, n-2, n)$ with $n \in (0, 1, 2, 3, \dots)$]. The radial size of the ϕ_{nm} 's is $\sim l = \sqrt{\hbar/m_e^* \omega_o}$, the characteristic length due to the lateral geometrical confinement in the dot, inclusive of the B field effects.

The corresponding single-particle energy levels are $\epsilon_{n,m} = (n+1)\hbar\omega_o - m\hbar\omega_c/2$. In the absence of SO , the full Hamiltonian for the dot, inclusive of the Coulomb interaction between the electrons (parametrized by U) is $H = \sum_{i=1}^N H_{(i)} + \sum_{i,j=1}^N U/|\vec{r}_i - \vec{r}_j|$. The orbital angular momentum M

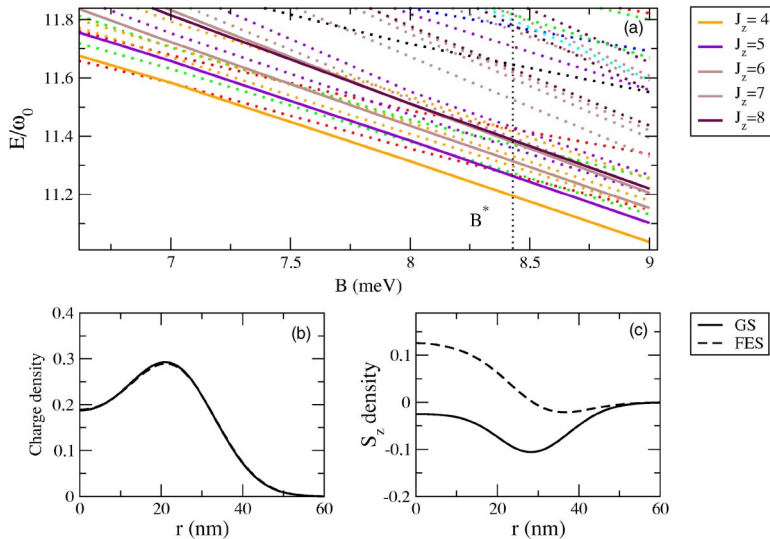


FIG. 3. (Color online) $N=4$ particles dot: (a) Energy spectrum vs magnetic field ω_c in the presence of the SO . The GS is $J_z=4$, the FES is $J_z=5$. $\omega_d=7$ meV, $U=13$ meV, $\alpha=250$ meV \AA . (b) The charge densities of the GS (black line) and of the FES (dashed line) of the FSP dot. (c) The corresponding spin densities of the GS (black line) and of the FES (dashed line) of the FSP dot.

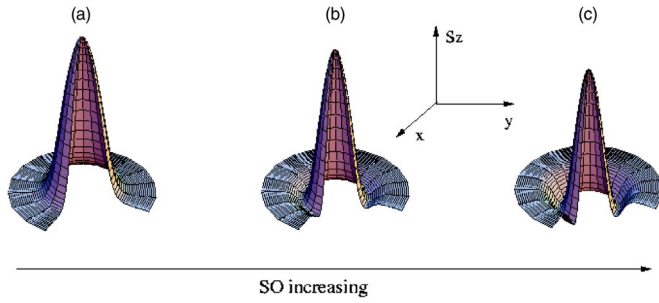


FIG. 4. (Color online) $N=3$ particles dot: FES spin density (arb. units) for (a) $\alpha=150$ meV \AA , (b) $\alpha=250$ meV \AA , (c) $\alpha=350$ meV \AA . By increasing the SO there is a squeezing close to the center and some reduction of $\langle \sigma_z \rangle$.

$=\sum_{i=1}^N m_{(i)}$, the total spin S and S_z (the projection of the spin along \hat{z}) are good quantum numbers.

By increasing \vec{B} , the dot undergoes a sequence of transitions to higher M and higher S states. These transitions have been monitored in the conductance for larger dots including tenths of electrons as well as for dots with few electrons.¹¹ Eventually, the GS reaches the maximum $M=N(N-1)/2$ and full spin polarization $S=N/2$ (MDD).^{13,14}

The confinement of the QD in the \hat{z} direction produces an electric field orthogonal to the dot plane, which gives rise to a Rashba term in the Hamiltonian that couples orbital and spin dynamics. In a biased dot the size of this perturbation would also depend on the screening of the source drain bias V_{sd} applied to the contacts. The single-particle Hamiltonian now reads

$$H_{(i)} \rightarrow H_{(i)} + \frac{\alpha}{\hbar} \left[\hat{z} \times \left(\mathbf{p}_i + \frac{e}{c} \vec{A}_i \right) \right] \cdot \vec{\sigma}_i. \quad (2)$$

Here $\vec{\sigma}$ are the Pauli matrices and α (measured in units of meV \AA) is the SO coupling parameter, which is proportional to the electric field in the \hat{z} direction. Good quantum numbers labeling the multiparticle states are now N , S , J_z , E , where $J_z=M+S_z$, the total angular momentum along z and E is the energy. Details of our exact diagonalization procedure have been reported previously.¹⁵

SO coupling lifts the spin degeneracy of the M multiplets, and the FSP GS attains the lowest J_z : $J_z^{FSP}=N(N-1)/2 - N/2$ (S_z is the projection of the spin along \hat{z}). In a previous paper, we exhibited the charge density and spin density of the first excited state (FES) (see Figs. 1 and 2), which showed unexpected spin-texture properties.¹⁴ Indeed, the FSP QD reproduces in a nutshell the quantum hall ferromagnet (QHF) at filling one, which has Skyrmion-like low-lying collective excitations.^{12,16,17} In Fig. 1(a) the lowest-lying energy levels E are plotted versus ω_c for $N=2$ with $\omega_d=5$ meV, $U=13$ meV and $\alpha=250$ meV \AA . The level structure is qualitatively analogous to that obtained in Ref. 18, intended for an InSb dot, with Dresselhaus and cubic SO terms included. The singlet-triplet transition appears here as a marked anticrossing at $\hbar\omega_c \approx 4$ meV, because of the SO coupling. The states involved in the anticrossing have $J_z=0$ and originate, in the absence of SO, from the singlet ($S=0, S_z=0, M=0$) and the triplet ($S=1, S_z=-1, M=1$) states.

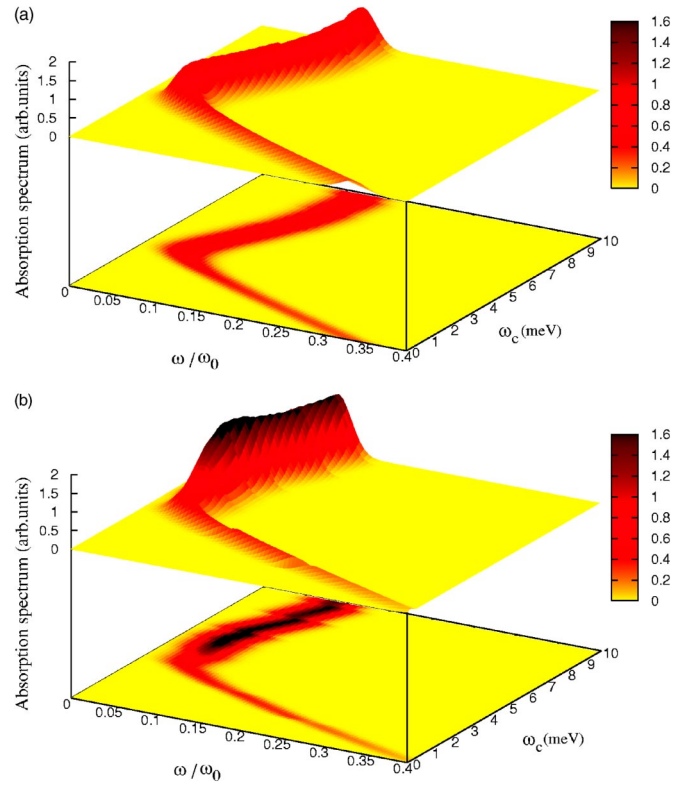


FIG. 5. (Color online) Absorption spectrum vs magnetic field for two (a), and four (b) particles. The excitation energies can be easily read from the contour-plot projection of the 3D surfaces onto the underlying plane.

Recently, the relaxation time T_1 for the flipping of the two-electron spin trapped in a vertical GaAs QD, from the triplet to the singlet state, has been measured, by applying electrical pulses to the QD. T_1 has been estimated to be $>200 \mu\text{s}$ at $T < 0.5$ K.¹⁹ Similarly to what found in Ref. 18, exchange interaction produces a small zero-field splitting between the first excited state (a triplet with $J_z=2$) and the second excited state (a singlet with $J_z=1$). Increasing B further, the SO induces the crossing of the latter two states, so that lowest-lying states are the GS ($S=1, J_z=0$) and the FES ($S=1, J_z=1$). This crossing qualifies B^* , which is rather insensitive to SO coupling.

As seen from Figs. 2 and 3, the same pattern can be found also for $N=3,4$. The SO coupling tends to shift the \uparrow spin density with regard to the \downarrow one radially.¹⁴ The shift can occur easily for the GS when $N=2$ and provides a reduction of the $e-e$ interaction by leaving an isolated spin at the center of the dot. When $N > 2$, the confinement potential together with the $e-e$ repulsion contrasts such a spin redistribution and the final result is that the z component of the total spin density is diminished at the center of the dot. In particular, $\sigma_z(r)$ tends to flatten in the GS for $N=3,4$. Correspondingly, the radial component $\sigma_r(r)$ increases in the case of $N=3,4$ at any distance from the center and not only at the dot boundary as it happens for $N=2$.

Anticrossings are less prominent for $N=4$ and the level of separation of the bunch of states in Fig. 3(a) is much smaller, but a gap develops at $\omega_c \approx 8.5$ meV, between the GS ($S=2, J_z=4$) and the FES ($S=1, J_z=5$). The gap is strongly sen-

sitive to the SO tuning and increases with increasing α [see Fig. 2(d) for $N=3$].

In the FES, the SO enforces a spin texture with $\langle S_z \rangle$ flipped at the origin with respect to the GS and healing back gradually away from the center up to the QD boundary, where the spin density points radially in the dot plane.¹⁴ The FES for $B > B^*$ has J_z increased by one with regard to the GS. This is mostly due to spin reversal because the difference of the angular momentum expectation values $\langle M \rangle_{FES} - \langle M \rangle_{GS}$ is found to be vanishingly small. In a disk-shaped dot, a radial change of $\langle M \rangle$ requires a change of $n(r)$ as well, but, as a matter of fact, we find that the charge distribution in the dot at the FSP point is rather insensitive to excitation and to the strength of the SO coupling [see Figs. 1(b), 2(b), and 3(b)]. While the radial charge density $n(r)$ appears to be compressible at fields $B < B^*$ and $B > B^*$, it is approximately incompressible at $B \sim B^*$. When $B \gg B^*$, the charge distribution of the dot reconstructs.^{14,20,21}

The spin excitation gives rise to an extra collective magnetization $\hat{z} \cdot \Delta \vec{M}(r) \approx \langle 2\mu_B \Delta \sigma_z(r) \rangle$, where $\Delta \sigma_z(r')$ is the difference in the z component of the local spin density between the FES and the GS and $\mu_B = e\hbar/2m_e c$. The radial spin density $\sigma_z(r)$ appears in Figs. 1(c), 2(c), and 3(c) for $N=2, 3, 4$ respectively.

We have estimated the possible extra magnetic flux ϕ associated to the spin excitation, by integrating numerically the vector potential, induced by the spin polarization of the dot, $a_\theta(r)$, along the circle of radius R at the dot boundary γ [$\phi = \int_\gamma R d\theta a_\theta(R)$]. This is given by

$$a_\theta(r) = \int_0^{2\pi} d\theta' \int_0^R \frac{dr' \vec{r}' \times \hat{z} \partial \Delta \mathcal{M}_z(r')}{|\vec{r} - \vec{r}'| \partial r'}, \quad (3)$$

where \hat{r} is a radial unit vector. The calculation yields a fraction of the flux quantum $\sim 10^{-5} hc/e$, but it is remarkable that, at $B \approx B^*$, we find the same value of ϕ for $N=2, 3, 4$. This is consistent with the fact that the FES has essentially one spin flipped at the origin and no change in orbital angular momentum.

FIR absorption. Far-infrared radiation is a common tool in large scale QD arrays [e.g., In QD's (Ref. 22) or field-effect confined GaAs QD (Ref. 23)]. In the presence of a Rashba SO term the center of mass coordinate and the relative coordinates are coupled together,²⁴ so that Kohn's theorem does not apply. It follows that FIR radiation could excite the many-body FES. We have calculated the dipole matrix element squared for the transition from GS to FES versus B . Our results are shown in Fig. 5 for $N=2$ (a) and $N=4$ (b), respectively. The dispersion of the absorption peaks is artificial, but their detailed shape would yield direct access to the coupling constants and to the relaxation mechanisms. We find an increase of the expected intensity at the FSP point, which marks the crossover to the new states. As expected, the crossover sharpens with increasing N .

Conclusion. Simultaneous application of an electric field with a magnetic field orthogonal to a disk-shaped QD reproduces the properties of a 2DEG QHF on the dot scale, with its Skyrmion excitations. SO opens an anticrossing gap above the GS and stabilizes a Skyrmion such as FES, within the gap, with a spin reversed at the origin of the QD. FIR can excite the dot, thus affecting nuclear magnetic resonance of underlying nuclear spins, as in recent experiments in GaAs quantum wells.²⁵

Discussions with S. Tarucha are gratefully acknowledged, as well as hospitality at ICTP, Trieste.

¹L. P. Kouwenhoven, D. G. Austing, and S. Tarucha, Rep. Prog. Phys. **64**, 701 (2001); L. P. Kouwenhoven and C. M. Marcus, Phys. World **116**, 35 (1998); M. A. Kastner, Ann. Phys. (N.Y.) **9**, 885 (2000).

²D. Loss and D. P. Di Vincenzo, Phys. Rev. A **57**, 120 (1998).

³B. E. Kane, Nature (London) **393**, 133 (1998).

⁴J. H. Smet *et al.*, Nature (London) **415**, 281 (2002).

⁵A. V. Khaetskii and Y. Nazarov, Phys. Rev. B **64**, 125316 (2001); Y. B. Lyanda-Geller, I. L. Aleiner, and B. L. Altshuler, Phys. Rev. Lett. **89**, 107602 (2002).

⁶E. I. Rashba, Fiz. Tverd. Tela (S.-Peterburg) **2**, 1224 (1960) [Sov. Phys. Solid State **2**, 1109 (1960)]; Y. A. Bychkov and E. I. Rashba, J. Phys. C **17**, 6039 (1984).

⁷J. Nitta *et al.*, Phys. Rev. Lett. **78**, 1335 (1997); D. Grundler, *ibid.* **84**, 6074 (1999).

⁸F. E. Meijer *et al.*, Phys. Rev. B **70**, 201307 (2004).

⁹J. B. Miller *et al.*, Phys. Rev. Lett. **90**, 076807 (2003).

¹⁰A. K. Hüttl *et al.*, Phys. Rev. B **69**, 073302 (2004).

¹¹T. H. Oosterkamp *et al.*, Phys. Rev. Lett. **82**, 2931 (1999).

¹²A. H. MacDonald, in *Quantum Transport in Semiconductor Heterostructures*, edited by B. Kramer (Kluwer, Dordrecht, 1996), p. 110.

¹³M. Stopa, Phys. Rev. B **54**, 13 767 (1996).

¹⁴P. Lucignano, B. Jouault, and A. Tagliacozzo, Phys. Rev. B **69**, 045314 (2004).

¹⁵B. Jouault, G. Santoro, and A. Tagliacozzo, Phys. Rev. B **61**, 10 242 (2000).

¹⁶S. L. Sondhi *et al.*, Phys. Rev. B **47**, 16 419 (1993).

¹⁷S. E. Barrett *et al.*, Phys. Rev. Lett. **74**, 5112 (1995); A. Schmeller *et al.*, *ibid.* **75**, 4290 (1995); E. H. Aifer, B. B. Goldberg, and D. A. Broido, *ibid.* **76**, 680 (1996).

¹⁸C. F. Destefani, S. E. Ulloa, and G. E. Marques, Phys. Rev. B **69**, 125302 (2004) (see Fig. 3).

¹⁹T. Fujisawa *et al.*, Nature (London) **419**, 278 (2002).

²⁰V. Gudmundsson *et al.*, Phys. Scr., T **69**, 150 (1997).

²¹L. P. Rokhinson *et al.*, Phys. Rev. Lett. **87**, 166802 (2001).

²²M. Fricke *et al.*, Europhys. Lett. **36**, 197 (1996); P. Junker *et al.*, Phys. Rev. B **49**, 4794 (1994).

²³R. Krahn, V. Gudmundsson, G. Heyn, and D. Heitmann, Phys. Rev. B **63**, 195303 (2001).

²⁴L. Jacak, P. Hawrilack, and A. Wójs, *Quantum Dots* (Springer-Verlag, Berlin, 1998).

²⁵G. Salis, D. T. Fuchs, J. M. Kikkawa, D. D. Awschalom, Y. Ohno, and H. Ohno, Phys. Rev. Lett. **86**, 2677 (2001); J. M. Kikkawa and D. D. Awschalom, Science **287**, 473 (2000).